

# Performance of a 1319 nm laser radar using RF pulse compression

Christopher Allen, Yanki Cobanoglu, Sekken Kenny Chong, Sivaprasad Gogineni

The University of Kansas, Radar Systems and Remote Sensing Laboratory

2335 Irving Hill Road, Lawrence, Kansas 66045-7612 USA

Telephone: 785 / 864-3017 Facsimile: 785 / 864-7789 email: callen@eecs.ukans.edu

**Abstract**—Spaceborne lidars have been shown to provide data on surface elevation, vegetation canopy heights, and aerosol characteristics. Satellites carrying lidars for measuring ice sheet surface elevation and vegetation canopy heights are scheduled to be launched in the next few years. To achieve the necessary resolution and sensitivity, lidars on these satellites will use short duration, high peak power transmit pulses. Because of their high peak power, these lidars must be operated with a low pulse repetition frequency (PRF). The high peak power operation results in limited lidar lifetime and the low PRF provides insufficient spatial samples along the satellite track.

To overcome these limitations of high peak power systems, at The University of Kansas we have developed a low peak power laser radar using modern RF techniques and fiber-optic technologies developed in support of the communication industry. We used RF pulse compression to achieve the sensitivity needed for spaceborne applications and have increased the PRF to provide more dense sampling. We have developed and reported (IGARSS'99 [1], '00 [2]) preliminary results of a fiber-optic-based, laser radar that applies RF pulse compression and digital signal processing techniques to improve receiver sensitivity and range measurement capabilities. With our improved super-heterodyne receiver, we have achieved receiver sensitivities below -100 dBm with transmit pulses with 40  $\mu$ s duration, 260 MHz bandwidth, and a 4 kHz PRF. These parameters are sufficient for altimeter operation from a satellite.

Over the last six months we have modified the receiver architecture, performed detailed system simulations, developed a new data acquisition system, and conducted laboratory tests to verify simulation results.

In this paper we will present the system design, results of performance analyses and tests. We will also show details on the two-stage down-conversion receiver with envelope detection and present issues concerning telescope-to-optical fiber coupling.

## INTRODUCTION

For altimeter systems, the key performance parameter is range accuracy,  $\sigma_R$ . Range accuracy is determined by the received signal bandwidth, B, and the signal-to-noise ratio, SNR [3,4].

$$\sigma_R = \frac{Kc}{B\sqrt{\text{SNR}}} \quad (1)$$

This relationship is only valid when  $\text{SNR} \gg 1$ . The value of the constant K depends on the type of algorithm applied. High peak power systems typically use short-duration pulses ( $\tau$ ) where  $B \approx 1/\tau$  with sufficient transmit power to provide the SNR needed to achieve the required range accuracy.

In our system, a long-duration ( $\tau = 40 \mu$ s), low peak power ( $< 1$  W) pulse is used to achieve a fine range accuracy ( $\sigma_R = 10$  cm). The transmitted pulse is modulated by a signal with a bandwidth commensurate with the desired range accuracy. With today's off-the-shelf fiber-optic components, multi-gigahertz bandwidth modulation is possible. While the signal parameter to be modulated could be frequency, phase, amplitude, or polarization, we selected amplitude modulation so that we could readily separate the modulation signal from the optical carrier in the receiver.

A chirp (or linear FM) waveform is used as the modulation signal [5]. This waveform consists of a sinusoid whose frequency varies linearly from  $f_1$  to  $f_2$ , where  $|f_1 - f_2|$  is the signal bandwidth, B. In our system, radio frequency signals are used,  $f_1$  is 100 MHz,  $f_2$  is 360 MHz, and B is 260 MHz. This chirp waveform is produced digitally using direct digital synthesis (DDS). As in conventional RF and microwave radar systems, once the chirp signal has been recovered in the receiver (in a process described below), the signal is dechirped (i.e., beat against the original RF chirp waveform), and low-pass filtered. The signal output from this process is a sinusoid of duration  $\tau$  and frequency  $f_R$  where

$$f_R = \frac{2BR}{c\tau} \quad (2)$$

and R is the range to the target. This signal is digitized and analyzed to determine R. An advantage of this approach is that while the signal bandwidth is 100s of MHz, the signal to be digitized may be only a few MHz, thus relaxing the requirements on the digitizing hardware.

## SYSTEM DESCRIPTION

Our system builds on the work reported by Mullen et al. [6], which combined microwave signals with optical carriers in a lidar application. In our laser radar system the transmitted optical signal and the reference for the local oscillator (LO) are obtained from a common laser. The signal to be transmitted is intensity modulated by the chirp waveform (modulation index  $\sim 100\%$ ) while the LO signal is frequency shifted by 600 MHz using an acousto-optic modulator (AOM). Following reception, the received signal is coherently downconverted to an intermediate frequency (IF) of 600 MHz. Following RF upconversion to about 3.6 GHz, the signal is envelope detected, then mixed with a baseband chirp signal, filtered, and digitized. A system block

diagram was presented in [2]. To provide the necessary optical signal power for both the transmitted signal as well as the LO signal, we have recently replaced the 5 mW, 1310 nm DFB laser with a more powerful 100 mW Lightwave Electronics that operates at 1319 nm and a linewidth of about 5 kHz.

Under normal operating conditions (large optical path loss), the output of the photodetector is shot-noise limited with an  $SNR \ll 1$ . Signal processing gains (pulse compression and coherent integration) are required to achieve the SNR required for accurate range measurement ( $SNR \gg 1$ ). Through digital signal processing, coherent integration and frequency analysis are applied to improve the SNR and determine  $f_R$  for range estimation. In coherent integration, digitized samples of previous echos may be averaged with the digitized representation of the latest echo to suppress the noise while preserving the signal. By averaging  $N$  echoes, this process provides an improvement in the SNR by a factor of  $N$ . Compared to a short pulse lidar (pulse duration of  $\tau$ ), pulse compression provides a signal-processing gain of  $T/\tau$  where  $T$  is the duration of the uncompressed pulse.

In envelope detection, which is accomplished through Schottky-barrier diode rectification, the envelope signal is recovered and the carrier signal is rejected. To perform envelope detection efficiently, the carrier frequency must be at least ten times greater than the maximum frequency of the envelope waveform, which is why we upconverted the signal to 3.6 GHz. Through envelope detection, we effectively discard the optical phase information and avoid many temporal correlation issues commonly associated with coherent laser remote sensing such as laser phase noise, atmospheric turbulence, and frequency shifting due to Doppler effects.

#### ENVELOPE DETECTION

For cases where the  $SNR \ll 1$ , the receiver system was designed to have a linear transfer characteristic; i.e., a 1 dB change in received optical signal power is translated into about 1 dB of change in the detected signal power and SNR. Experimental tests have validated the linearity of the receiver up to the envelope detector input. To determine the transfer characteristic of the envelope detector for the  $SNR \ll 1$  case we used simulations, experiments, and analysis.

The envelope can be thought of as sidebands about the RF carrier. The square law characteristic of the detector generates a term, which is a product of the carrier, and the sideband, which is the baseband version of the envelope signal. In our noise-dominated condition, noise is also mixed with the carrier and sidebands, effectively increasing the noise power. Consequently, during envelope detection the SNR is degraded by about 10 dB. In addition, since both the carrier and the sidebands are attenuated by the optical losses, the product of these two terms is affected doubly by the optical path loss. Consequently the envelope detector has a nonlinear transfer characteristic.

Detected SNR versus optical signal power was measured in the laboratory replacing the circulator, telescope, optical amplifier, and bandpass filter with a variable optical attenuator. Fig. 1 (top) shows measured data. The system parameters used in this experiment are shown within the figure. A linear least-squares fit of the data has a slope of 1.23, which we attribute to the nonlinearities of envelope detection. The LO power (0 dBm) represents the power level input to the polarization diversity receiver.

#### DIRECT DOWNCONVERSION

As an alternative to envelope detection, we have investigated direct downconversion of the RF signal to baseband. Rather than mix the photodetected RF signal up to 3.6 GHz, we mix it down to baseband where it is dechirped and processed as before. This approach should provide a more linear transfer characteristic than envelope detection.

Laboratory measurements of this system implementation were made using the same test setup described for the previous case. The results are shown in Fig. 1 (bottom).

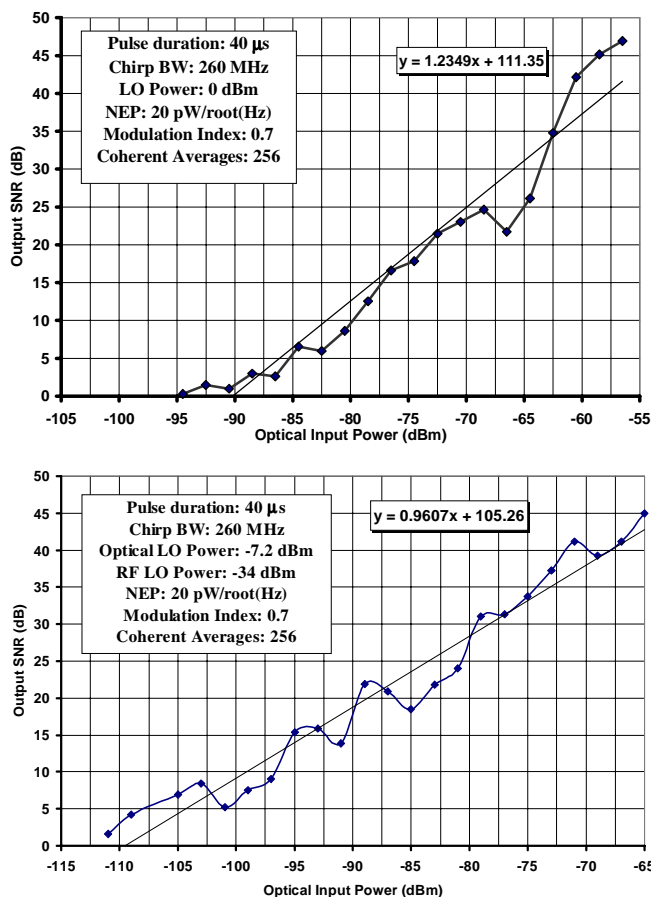


Fig. 1. Measured SNR output from the receiver signal processor versus optical signal power input to the polarization diversity receiver. Top: Envelope detection using a Schottky-barrier diode. Bottom: Direct downconversion.

The linear least-squares fit has a slope of 0.96 indicating a more linear transfer characteristic. In addition, although the optical LO power is lower than in the previous case, the sensitivity of the receiver is greater than before by about 10 dB. The increased sensitivity is attributable to the fact that the 10 dB SNR degradation of the envelope detection is avoided and to the fact that a relatively strong (-34 dBm) RF local oscillator is present to downconvert the chirp sidebands.

A drawback to direct downconversion exists, however. In direct downconversion the perturbations of the optical frequency and phase remain in the detected signal. The phase stability of the detected signal, both intrapulse and pulse-to-pulse, is now impacted by laser phase noise, atmospheric turbulence, Doppler effects, etc. These pulse-to-pulse phase variations of the dechirped pulse may preclude the use of coherent integration to further boost the SNR.

#### FIBER-TO-TELESCOPE INTERFACE ISSUES

The transition from guided waves (in the single-mode optical fiber, SMF) to free space via the telescope requires care. Astronomers demonstrated the feasibility of coupling SMF to large aperture telescopes in the 1980s [7,8]. They showed that the maximum theoretical coupling efficiency is about 80% (or 1 dB) due to mismatches in the field distribution between the telescope and the fiber. When applied to lidar applications, the maximum coupling efficiency may be only about 42% (-3.8 dB) when random light is coupled into SMF [9].

For efficient coupling efficiencies, the numerical aperture, NA, of the telescope must match that of the fiber. The NA of SMF (designed for operation at wavelengths of 1.3 to 1.5  $\mu\text{m}$ ) is about 0.11, which corresponds to an f/ratio of 4.5 using

$$f / \text{ratio} = (2 \text{ NA})^{-1} \quad (3)$$

For optimum coupling to SMF, the telescope's f/ratio should be between 7.6 and 3.3 [8]. The Celestron 5 in (127 mm) diameter Schmidt-Cassegrain telescope we used has an f/ratio of 10, which corresponds to an NA of 0.05. To improve the NA matching, we used a focal reducer to convert the telescope's f/ratio to f/5. Also, the clear aperture blockage for this telescope is about 16 %, due to the secondary mirror.

The fiber-to-telescope interface consists of a bare, polished fiber end placed in the telescope's focal plane. We mounted an FC/PC connector sleeve on a fixture on the rear cell of the telescope so that a simple SMF patch cord could be readily attached to deliver the light to the telescope. One drawback of this solution is the 4% (-14 dB) reflection at the fiber/air interface. When operated in monostatic mode, the transmit signal reflection from the fiber end may overwhelm the receiver and mask the weak return signal. To avoid this back reflection, an FC/APC fiber termination can be used; however, due to the 8° launch angle, the radiated light will be skewed by about 3.4° off axis. This can be overcome with an optical wedge between the APC fiber launch and the telescope.

To assess the coupling efficiency of our fiber-to-telescope interface, we used two identical 5 in telescopes, each with an FC/PC terminated fiber in the focal plane. An insertion loss of about 12 dB (compared to a fiber-to-fiber connection) was measured when the two telescopes were aligned and their beams collimated. Hence the efficiency of our fiber-to-telescope interface is approximately 25% (-6 dB).

#### SUMMARY

The feasibility of using RF pulse compression and coherent averaging to enhance receiver sensitivity has been demonstrated. Doubling the transmitted pulse duration doubles the detected SNR, as does doubling the number of coherent integrations. While envelope detection has a nonlinear transfer characteristic and degrades the SNR by 10 dB when the signal is dominated by noise, it has the advantage of discarding the effects of optical frequency and phase variations on the detected signal. Direct downconversion has a more linear transfer characteristic, yet the effects of the optical signal's frequency and phase remain in the detected signal. Our simple fiber-to-telescope interface provides a 25% coupling efficiency.

#### ACKNOWLEDGMENTS

This work is funded by the NASA Earth Science Enterprise's Instrument Incubator Program contract number NAS1-99052.

#### REFERENCES

- [1] C. Allen and S. Gogineni, "A fiber-optic-based 1550-nm laser radar altimeter with RF pulse compression," *Proceedings of the 1999 International Geoscience and Remote Sensing Symposium (IGARSS '99)*, Hamburg, Germany, pp. 1740-1742, June 1999.
- [2] Allen, C., Y. Cobanoglu, S. K. Chong, and S. Gogineni, "Development of a 1310-nm, coherent laser radar with RF pulse compression," *Proceedings of the 2000 International Geoscience and Remote Sensing Symposium (IGARSS '00)*, Honolulu, Hawaii, pp. 1784-1786, July 2000.
- [3] Skolnik, M. I., "Theoretical accuracy of radar measurements," *IRE Transactions on Aeronautical and Navigational Electronics*, pp. 123-129, Dec. 1960
- [4] Jelalian, A. V., *Laser Radar Systems*, Artech House, Norwood, Massachusetts, p. 45, 1992.
- [5] Kachelmyer, A. L., "Range-Doppler imaging: wave-forms and receiver design," *Laser Radar III*, R.J. Becherer, Ed., Proc. SPIE, vol. 999, pp. 138-161, 1988.
- [6] Mullen, L.J., A.J.C. Vieira, P.R. Herczfeld, and V.M. Contarino, "Application of RADAR technology to aerial LIDAR systems for enhancement of shallow underwater target detection," *IEEE Transactions on Microwave Theory and Techniques*, 43(9), pp. 2370-2377, 1995.
- [7] Shaklan, S. "A long-baseline interferometer employing single-mode fiber optics," *Fiber Optics in Astronomy -- Vol. 3*, S.C. Barden, Ed., pp. 262-268, 1988.
- [8] Shaklan, S. and R. Roddier, "Coupling starlight into single-mode fiber optics," *Applied Optics*, 27(11), pp. 2334-2338, 1988.
- [9] Winzer, P.J., and W.R. Leeb, "Fiber coupling efficiency for random light and its applications to lidar," *Optics Letters*, 23(13), pp. 986-988, 1998.